Int J Adv Manuf Technol (2017) 88:1089–1099
DOI 10.1007/s00170-016-8838-3

ORIGINAL ARTICLE

Experimental investigation into the effect of low plasticity burnishing parameters on the surface integrity of TA2

Xilin Yuan[1] · **Yuwen Sun**[1] · **Chunyan Li**[2] · **Weirui Liu**[1]

Received: 13 September 2015 / Accepted: 25 April 2016 / Published online: 5 May 2016

Abstract The surface integrity of a titanium workpiece is closely related to its surface quality and performance. In order to improve the surface integrity, low plasticity burnishing is adopted. In this study, the effects of burnishing pressure (5–20 Mpa), speed (50–600 mm/min) and feed rate (0.05–0.5 mm) on the surface integrity are studied by single factor experiments. Four aspects of the surface integrity are investigated, namely surface roughness, surface microhardness, surface residual stresses, and surface topography. The results show that increasing the burnishing pressure or number of passes can improve the surface microhardness and the residual stress. However, increasing the burnishing pressure or number of passes contributes to reducing the surface roughness. Increasing the feed rate also leads to an increase in the surface roughness. Decreasing the burnishing speed is beneficial for increasing the surface residual stress. The analysis results of power spectral density profiles reveal that the burnishing pressure and feed rate are the dominant factors on the surface topography of the burnished workpieces. The surface residual stress changes from −67.7 Mpa to −400.5 Mpa after the burnishing process. The surface roughness reaches the minimum value of 0.057 μm at the feed rate of 0.05 mm. There is nearly a 36 % increase in the surface microhardness as compared to that of the unburnished workpiece. It shows that low plasticity burnishing can efficiently improve the surface integrity of a titanium workpiece.

Keywords Low plasticity burnishing · Surface integrity · TA2

✉ Yuwen Sun
xiands@dlut.edu.cn

[1] Key Laboratory for Precision and Non-Traditional Machining Technology of the Ministry of Education, Dalian University of Technology, Dalian 116024, China

[2] School of Material Science and Engineering, Dalian University of Technology, Dalian 116024, China

1 Introduction

Titanium alloy is widely used in various industries, such as aerospace industries, biomedical, chemical, resource, and power fields, due to its series of features, such as high plasticity, excellent forming process performance, and excellent corrosion resistance. However, this kind of alloy is difficult to machine due to its superior performance. During the machining process, high toughness of titanium alloy leads to high cutting temperatures. Moreover, the continuous curled chips can easily wrap around the tool, which gives rise to an excessive tool wear during the machining process, thereby deteriorating the surface integrity. Then, the performance and service life of the workpieces are affected. Therefore, in order to improve the surface integrity, surface treatments are needed for their practical applications.

Low plasticity burnishing (LPB) is a novel surface treatment process which has attracted a considerable attention lately. Figure 1 illustrates the schematic of a LPB tool. This tool can be easily mounted onto the spindle of the milling machine, like a milling cutter. Burnishing pressure is provided by a hydraulic pump. The hydraulic oil works as the power source and coolant as well as lubricant. The ceramic ball is pressed against the surface of the workpiece. The ball can freely rotate on the workpiece surface. Under the pressure of the hydraulic oil, the plastic deformation is produced on the workpiece surface. The materials flow from the peaks to the valleys. As a

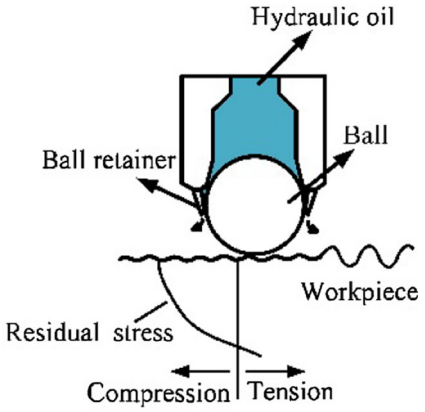

Fig. 1 Schematic of low plasticity burnishing

result, the workpiece surface is smoothed after the LPB process. Meanwhile, a layer of residual compressive stress is induced with a concomitant hardening of superficial materials due to plastic deformation.

Several studies have been concentrated on the effects of ball burnishing process on the surface integrity of different materials. Gharbi et al. studied the effect of ball burnishing process on the surface quality of AISI 1010 steel plates. Results showed that surface roughness decreased at first and then increased with the burnishing speed further increasing. However, the burnishing feed rate almost had no effect on surface roughness [1]. Zhang et al. found that surface roughness increased with increasing burnishing feed or pressure [2]. Burnishing speed had little effect on the surface roughness. For hardened steels, Luca et al. found that roughness decreased with increasing pressure [3]. Burnishing was also applied on a lathe. Okada M et al. found that the main process parameters affecting the burnished surface integrity were burnishing force and feed rate, whereas the influence of the burnishing speed was minimal [4].

Several studies have been undertaken to investigate the effects of ball burnishing parameters on residual stress and surface hardening. For the improvement of surface hardness, Rao et al. reported that an improvement of about 30–45 % in surface hardness of dual-phase steels can be obtained by ball burnishing process [5]. Also, Loh et al. showed that an improvement of about 33–55 %, can be obtained by the ball burnishing of AISI 1045 steel process [6]. The results from Abdulstaar et al. showed that the surface hardness increased from 100HV0.05 to 150HV0.05 after the ball burnishing of AA5083 alloy [7]. However, for some relatively high-hardness materials, the ball burnishing process cannot significantly improve the hardness of the workpiece. Hamadache et al. obtained a 7 % surface hardness improvement via the ball burnishing of 36CrNiMo6 steel process [8]. Sequera et al. investigated the surface integrity of Inconel 718 by ball burnishing [9]. The results showed that there was nearly 14 % increase in the surface hardness after the ball burnishing process. Similarly, Zay et al. found that hardness increased from 370HV0.1 to 425HV0.1, an improvement of about 15 %, after the ball burnishing process [10]. Besides, the residual stresses increased from −200 Mpa in the surface layer to −800 Mpa at 200 μm below the surface. The residual compressive stress was up to 70 % of the material yield strength.

For the residual stresses generated in the ball burnishing process, some researchers carried out experimental studies. In [11], the maximum magnitude of the compressive residual stress, produced by deep cold rolling the specimens of the titanium alloys Ti-6Al-4 V, reached up to −1000 to 1200 Mpa. In addition, the depth of compressive residual stress was up to 0.6 mm. Prevéy et al. reported that the maximum compression was approximately −480 MPa between the surfaces and a depth of nominally 0.2 mm was obtained by LPB processing of AA7075-T6 [12]. Several researchers studied the residual stress induced by the ball burnishing process utilizing the finite element method (FEM) [13–17]. The advantage of FEM is being able to predict the material state after burnishing without having to conduct large-scale physical tests. However, the maximum depth of the residual stress layer after the ball burnishing process is about 1 mm. In this depth of a 1-mm region, the residual stress dramatically changes. The dramatic changes in the residual stress and complex contact conditions require high-density finite elements. As a result, an exact FEM model is required for reducing the errors between the simulation results and the actual values.

An improvement of surface integrity will enhance the corrosion and fatigue behavior of the burnished specimen. Avilés et al. found that the fatigue limit of the burnished specimen increased by 21.25 % [18]. Gharbi et al. investigated the effect of burnishing force on the surface quality and on the service properties of rolled sheets of AISI 1010 steel [19]. Experimental results showed that the flat burnishing surfaces did not improve the fatigue strength of AISI1010 steel flat specimens. Mansour Mhaede obtained pronounced enhancement in the fatigue life tested

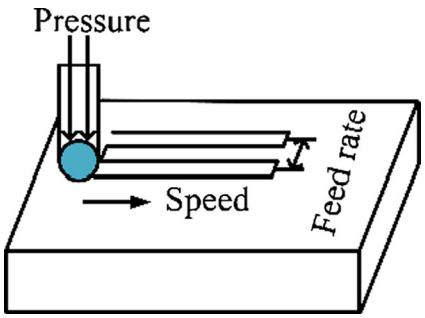

Fig. 2 Schematic of ball burnishing parameters

Table 1 The chemical composition of TA2 (in wt. %)

Fe	C	N	O	H	Ti
0.3	0.1	0.05	0.25	0.0015	Rest

in ambient air as well as corrosion fatigue life tested in 3.5 % NaCl after both shot peening and ball burnishing compared to the electrolytically polished reference conditions [20]. The improvement in fatigue is attributed to the combined actions of a layer of compressive residual stress, a high-quality surface finish, a reduction of the grain size in the surface zone, and an increase in the surface hardness. As a result, the fatigue crack initiation and propagation are suppressed.

As aforementioned, it was found that the effect of the burnishing process on the surface integrity of TA2 alloy is seldom studied. Therefore, the objective of this work is to systematically investigate the effects of process parameters on surface integrity in burnishing of TA2 alloy. In this study, the effects of four parameters (Fig. 2) on surface roughness and surface microhardness as well as residual stress are investigated. Besides, when the surface is smooth enough, the traditional evaluation index of surface topography is not suitable. The power spectral density method was adopted to characterize the burnished surfaces. The results will be beneficial for optimization of the LPB process parameters for TA2 alloy.

2 Experimental procedure

2.1 Workpiece material

The material selected in the present study is TA2 alloy. The composition and mechanical properties of TA2 alloy are listed in Tables 1 and 2, respectively. Before the burnishing process, titanium plates were prepared in the dimension of 30 mm × 20 mm × 5 mm. The finish milling parameters are listed in Table 3.

2.2 Milling and burnishing tools

Twenty-five workpieces were machined with an end mill on a Haas machining center (VF-5/40XT). The Ecoroll HG6 burnishing tool is utilized in this study, which has a 6-mm diameter nitride ceramic ball (Fig. 3). The hydraulic pressure is controlled by the Ecoroll HGP3.0 hydraulic unit. This unit can provide the maximum pressure of 20 Mpa.

Table 2 The mechanical properties of TA2

Density (g/cm^3)	Tensile strength (Mpa)	Yield strength (Mpa)	Modulus of elasticity (Gpa)	Hardness (HV)
4.5	654	577	107.8	190

Table 3 Experimental conditions during finish milling TA2 alloy

Spindle speed (rpm)	1500
Feed (mm/min)	150
Depth-of-cut (mm)	0.2

2.3 Experimental design

Experiments were carried out to investigate the effects of burnishing parameters on the surface integrity characteristics of TA2 alloy. Based on the principle of single factor experiments, each set of experiments has different combinations of burnishing parameters. Only one burnishing parameter varied and the others were kept constant in each set of experiments. The burnishing pressure was set to 5–20 Mpa. The feed rate varied from 0.05 to 0.5 mm. The burnishing speed was varied in the range 50–600 mm/min. The number of passes was set to one to five. Table 4 shows the design for the four sets of experiments in detail.

2.4 Measurement

The surface roughness was measured by Zygo New View 5022 scanning white light interferometer (SWLI). The surface microhardness was measured with an HXD-1000TM microhardness tester under a load of 98 g with a dwelling time of 15 s. Final surface roughness value and microhardness value were obtained from the mean value of five different positions on the surface. The mean value of the surface roughness of the milling machined workpiece was 0.51 μm (Ra). Surface topography of the workpieces was measured using a contact probe surface profiler (Form Talysurf PGI 840, Taylor Hobson, Leicester, UK). Surface residual stress was examined by X-ray diffractometry (XRD, PANAlytical Empyrean, CuKα radiation). The microstructure was investigated by MeF3 optical metalloscope.

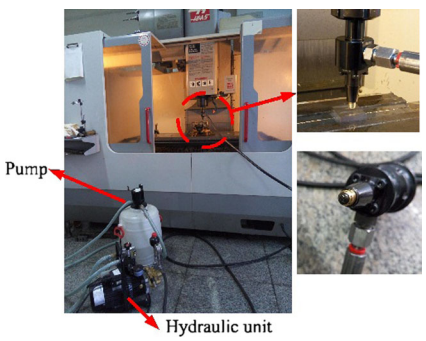

Fig. 3 Low plasticity burnishing tool

Table 4 Burnishing experiment design

	Number	Pressure P (Mpa)	Feed rate F (mm)	Number of passes N	Speed V (mm/min)
Pressure	1	5	0.2	1	100
	2	10	0.2	1	100
	3	15	0.2	1	100
	4	20	0.2	1	100
Feed rate	5	15	0.05	1	300
	6	15	0.1	1	300
	7	15	0.2	1	300
	8	15	0.3	1	300
	9	15	0.4	1	300
	10	15	0.5	1	300
Speed	11	14	0.2	1	50
	12	14	0.2	1	100
	13	14	0.2	1	150
	14	14	0.2	1	200
	15	14	0.2	1	250
	16	14	0.2	1	300
	17	14	0.2	1	350
	18	14	0.2	1	400
	19	14	0.2	1	500
	20	14	0.2	1	600
Number of passes	21	14	0.2	1	300
	22	14	0.2	2	300
	23	14	0.2	3	300
	24	14	0.2	4	300
	25	14	0.2	5	300

3 Results and discussion

3.1 Surface roughness

Figure 4 shows the effect of burnishing pressure on the surface roughness. The surface roughness decreased with the increase of the burnishing pressure. When the pressure reached to 20 Mpa, the surface roughness dropped to around 0.2 μm (Ra). At a given ball size, according to Hertz theory of elastic contact, a higher burnishing pressure leads to a higher contact radius. With the increase of depth, the contact stress is reduced. As seen from Fig. 5, it is evident that a gradient structure in terms of grain size developed at the near surface region. With the increase of distance from the surface, the magnitude of plastic deformation decreases. As a result, the size of the grain is on the increase with the increase of distance from the surface.

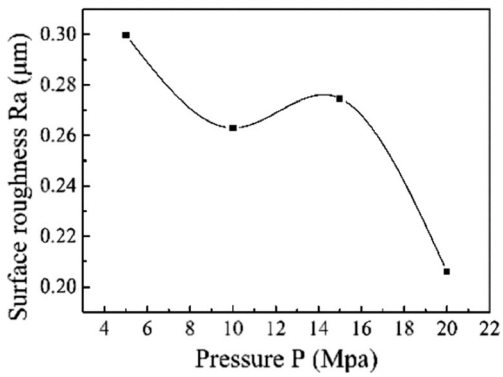

Fig. 4 Effect of pressure on surface roughness

As shown in Fig. 6, the smaller feed rate, the smoother the burnished surface will be. The value of surface roughness decreased from 0.508 to 0.057 μm (Ra) at the feed rate of 0.05 mm. The smaller feed rate produces lower residual area, which in turn produces a smoother surface.

Figure 7 depicts the effect of the burnishing speed on the surface roughness. When the speed increased from 50 to 600 mm/min, the surface roughness fluctuated between 0.202 and 0.268 μm (Ra). Obviously, burnishing speed has a little effect on the surface roughness.

Figure 8 shows the effect of the number of passes on the surface roughness. The surface roughness decreased with the increase of the number of passes. The minimum surface roughness decreased to 0.183 μm (Ra). Compared with the burnishing pressure, the improvement effect of the number of passes on the surface roughness is more obvious. Increasing the number of passes, the burnishing tool will have more chances to smooth the highest peaks and deepest valleys of

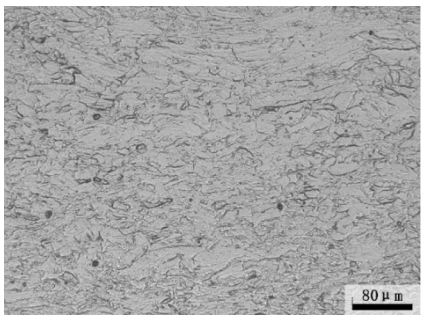

Fig. 5 Cross-sectional macrograph of ball burnished zone (P = 20Mpa, F = 0.2 mm, V = 100 mm/min, N = 1)

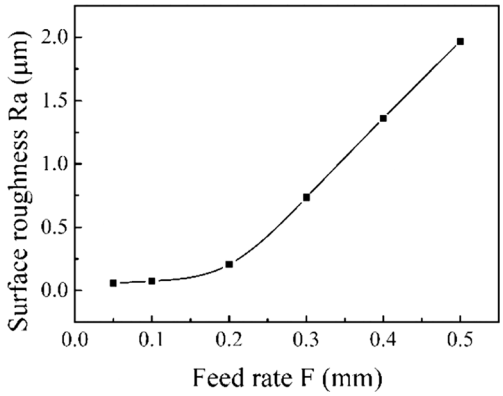

Fig. 6 Effect of feed rate on surface roughness

the workpiece. As a result, the surface roughness will be reduced.

3.2 Surface microhardness

Since the microhardness value is sensitive to the dislocation density of plastic deformation, it can be indirectly evaluated by the existence of compressive residual stress and surface-hardening layer. High density in the deformed surface layer will results in high surface hardness. Figure 9a shows the profile of surface microhardness induced by a different burnishing pressure. The surface microhardness kept increasing with the increase of burnishing pressure. The surface microhardness increased by 36.8 %, compared to the initial surface microhardness. However, when the feed rate varied between 0.05 and 0.1 mm, surface microhardness did not get the maximum (Fig. 9b). Only when the feed rate increased to 0.2 mm, the surface microhardness was significantly improved. But when the feed rate exceeded 0.3 mm, the surface microhardness began to decrease. This may be attributed to the fact that the burnishing feed rate was the same with the feed per revolution of the milling process. As a result, the rolling ball has more opportunities to push the material from the peaks to the valleys. A hard layer occurred on the workpiece surface. When the burnishing speed was relatively small (Fig. 9c), the surface microhardness was improved obviously. This may be attributed to the fact that the roller had more time to push the bulk material from the peaks to the valleys, leading to an increase in the amount of plastic deformation. Consequently, an increase of the surface microhardness can be observed. As shown in Fig. 9d, when the number of passes was less than three, the surface microhardness value was almost the same. When the number of passes reached four times, the surface microhardness increased significantly. However, when the number of passes exceeded four, the surface microhardness began to decrease. This may be attributed to the fact that serious work hardening may be formed in the material of "peak" when the number of passes was less than four. The crack initiation and propagation occurred in the work-hardened "peak" with further number of passes, which result in the formation of the surface spalling. As a result, the surface roughness was deteriorated and the surface microhardness began to decrease.

3.3 Surface residual stress

As seen from Fig. 10a, the surface residual stress increased with the increase of the burnishing pressure. The maximum compressive residual stress reached to −340 Mpa. The initial surface residual stress of the milled workpiece was −67.7 Mpa. As seen from Fig. 10b, the surface residual stress increased at first and then decreased with the feed rate further increasing. The maximum surface residual stress was −400.5 Mpa with the feed rate of 0.2 mm. Obviously, the smaller feed rate was not able to get the larger surface residual stress. Only when the burnishing feed rate was close to the feed per revolution in the milling process, the maximum surface residual stress could be obtained. In this case, the ball will have more opportunities to push the material from the peaks to the valleys. As seen from Fig. 10c, a higher surface residual stress can be observed at lower burnishing speed. Surface residual stress increased with the increase of the number of passes. By comparing Fig. 10a, d, it can be found that the effect of the number of times on the residual stress was much

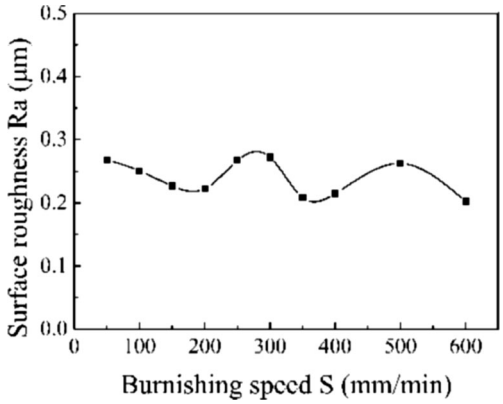

Fig. 7 Effect of burnishing speed on surface roughness

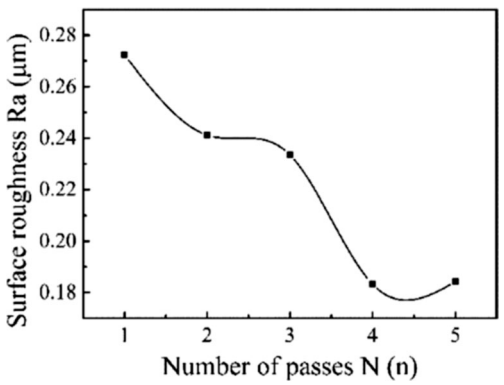

Fig. 8 Effect of number of passes on surface roughness

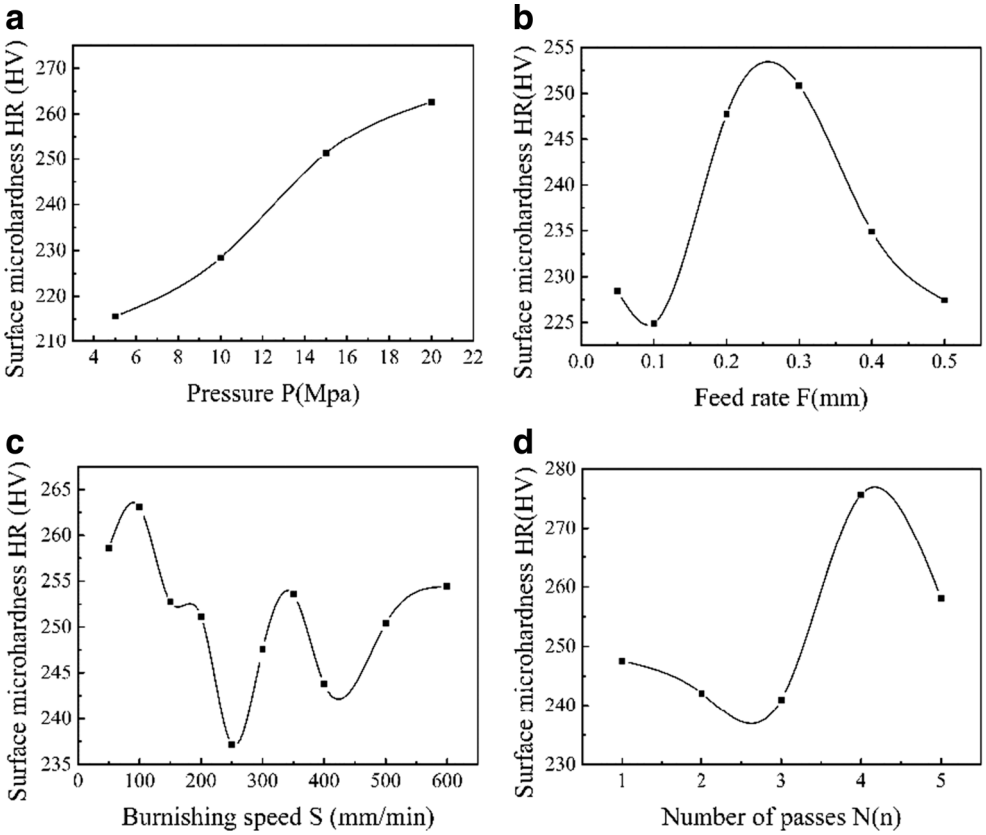

Fig. 9 Effect of burnishing process parameters on surface microhardness

more obvious. As more roughness valleys were "filled" during the process, the increase of the number of passes may lead to more plastic deformation. Each pass is a repetition of rolling the surface of the workpiece along the same trajectory under

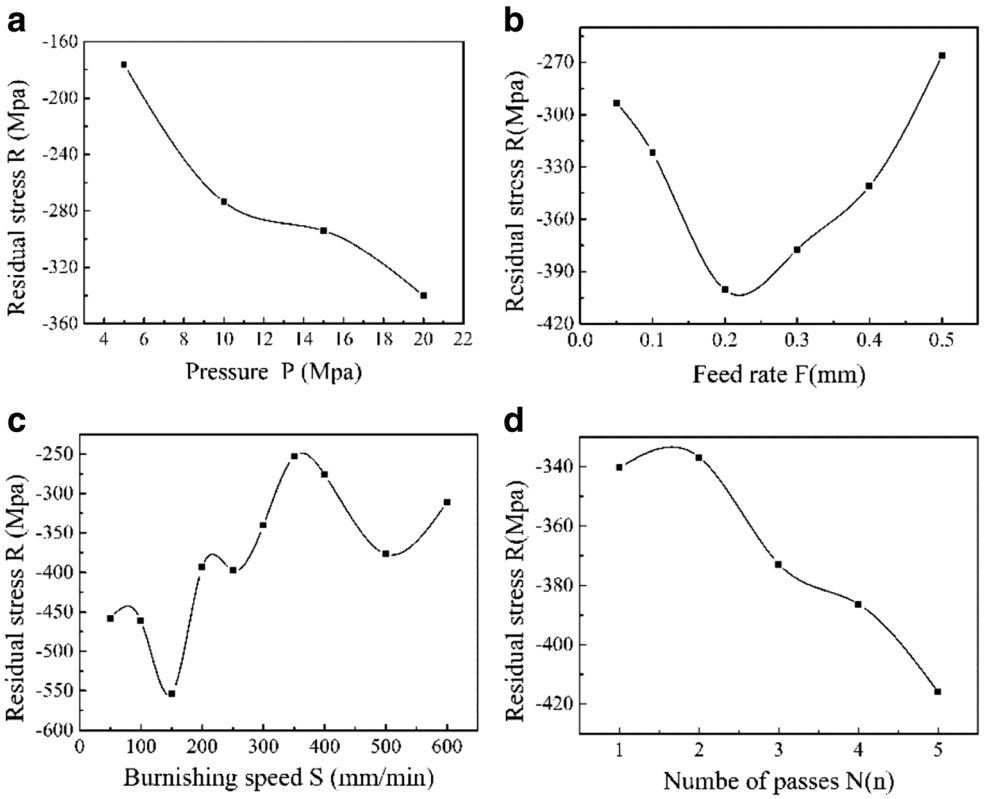

Fig. 10 Effect of burnishing process parameters on surface residual stress

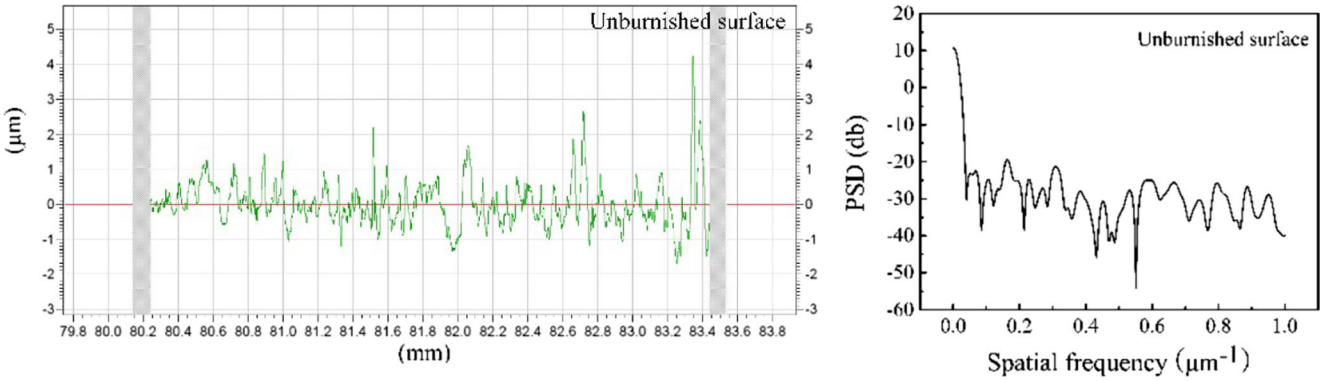

Fig. 11 Surface topography (L) and power spectral (R) density for initial milling surface

the same pressure. In this sense, the ball surface is smooth or not directly related to the surface roughness of the burnished workpiece. With the increase of the number of passes, much more elastic and elastic plastic deformation of the material of the workpiece surface were transferred into plastic deformation, which in turn refined the grains of the surface layer. As a result, an obvious improvement of the surface residual stress was observed.

3.4 Surface topography

The surface topography of the machined surface has great influence on the mechanical properties, especially wear, friction, and lubrication. Studies on mechanical processing surface topography indicated that with the continuous improvement of measurement resolution, the surface topography exhibited self-similarity. Traditional evaluation parameters of roughness such as Ra, Rq, and Rz, only characterize the changes in surface topography height, and the information of the spatial parameters are not included. The surface profile can be regarded as a random signal, which is composed of numerous different cycles of the sine curve, so it is continuous in the frequency domain. The sum of random signal in the frequency domain is one. Power spectral density (PSD) reflects the strength of a certain frequency band in a random signal. The power spectral density of the surface profile is calculated by Fourier transformation of the acquired digital signal of surface micro-profile, followed by multiplying the square of the resulting spectrum with the sampling density. The power spectral density of the ball burnished surface can be distinguished

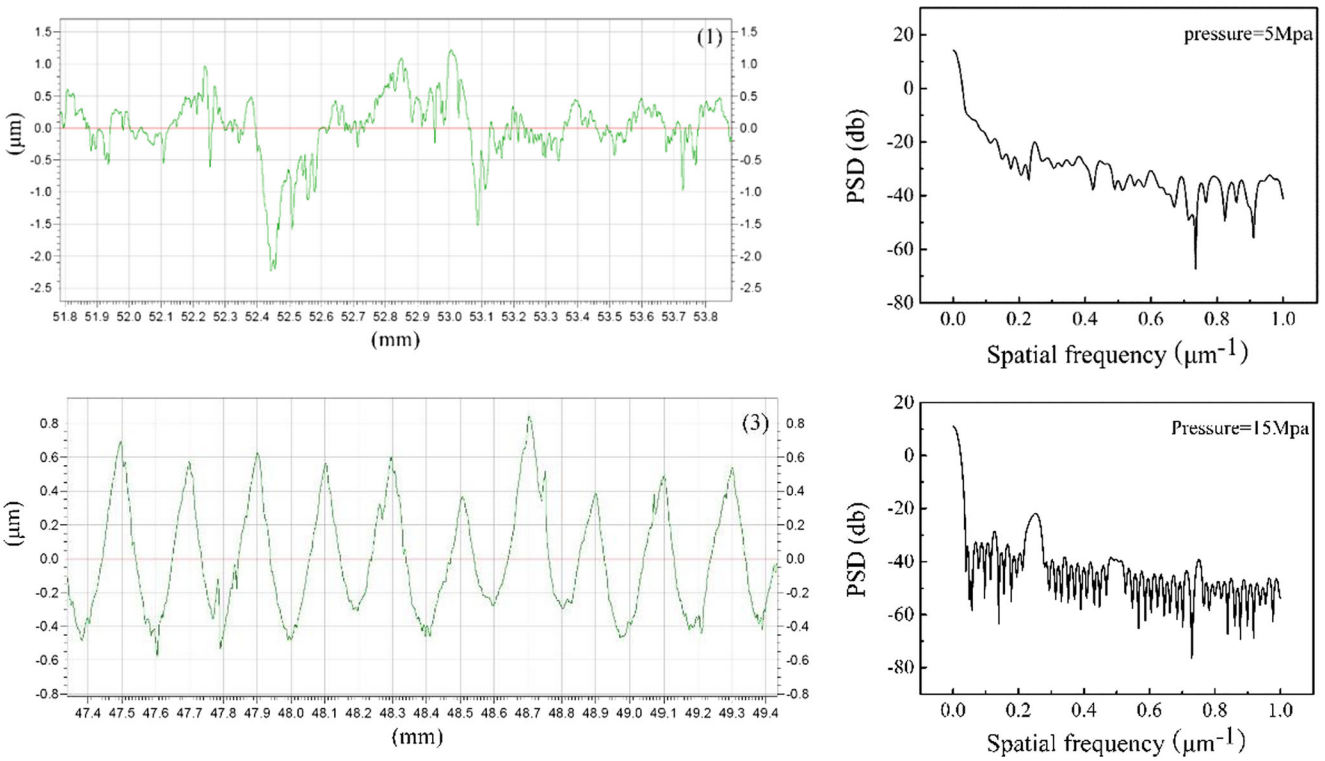

Fig. 12 Effect of pressure on the surface topography (L) and the power spectral (R) density

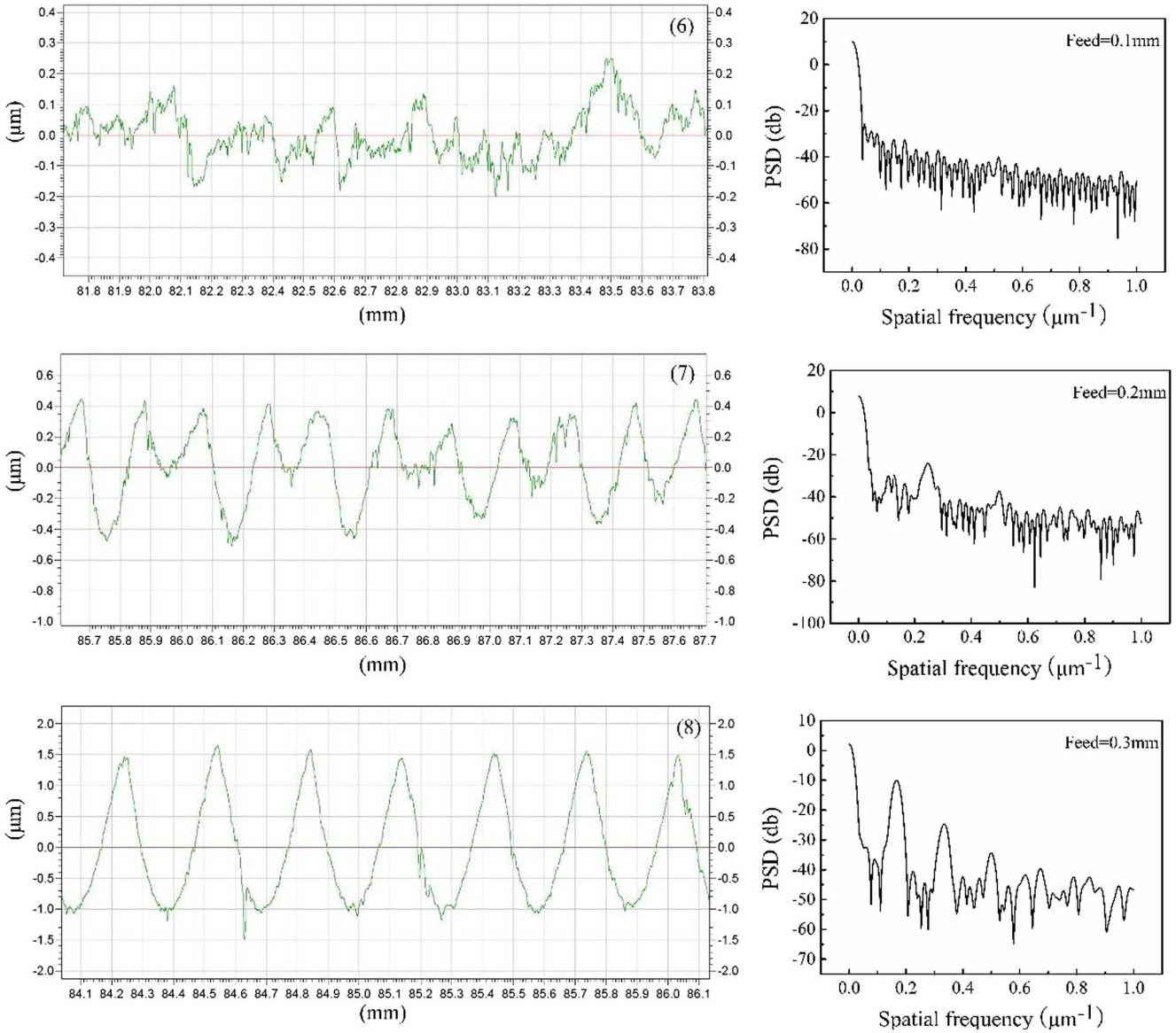

Fig. 13 Effect of feed rate on the surface topography (L) and the power spectral (R) density

by the different spatial frequency components contained in the surface profile, and it can be used to evaluate the influence of the different spatial frequency components on the surface microstructure.

Figures 11 and 12 show the surface topography and power spectral density of the burnished and unburnished surface. As is shown in the surface topography graph, the distance between the peaks and valleys is relatively large before burnishing. After the burnishing process, the distance between the peaks and valleys significantly reduced, emerged cyclical peaks and valleys. As seen in PSD graph, the amplitude of the power spectral density curve is larger at low frequencies, and the power spectral density curve is attenuated at high frequencies. After ball burnishing, the peak value of the low frequency and high frequency segments of the original milling surface are decreased, suggesting that the entire surface topography is improved. As the pressure increases, the power spectral density of the low frequency region is small, almost linear. In other words, based on fractal theory, when the frequency is below 0.1 μm^{-1}, the surface topography of the workpieces of the burnished surface is periodic. The peak of power spectrum density of the low frequency region is relatively high, which is mainly due to the feed rate of the milling process.

Figure 13 shows the effect of burnishing feed rate on the surface topography and power spectral density of the burnished surface. When the feed rate was lower than 0.2 mm, the amplitude of the power spectrum density of the high frequency region was relatively small. When the feed rate was more than 0.2 mm, the amplitude of the power spectrum density of the high frequency region

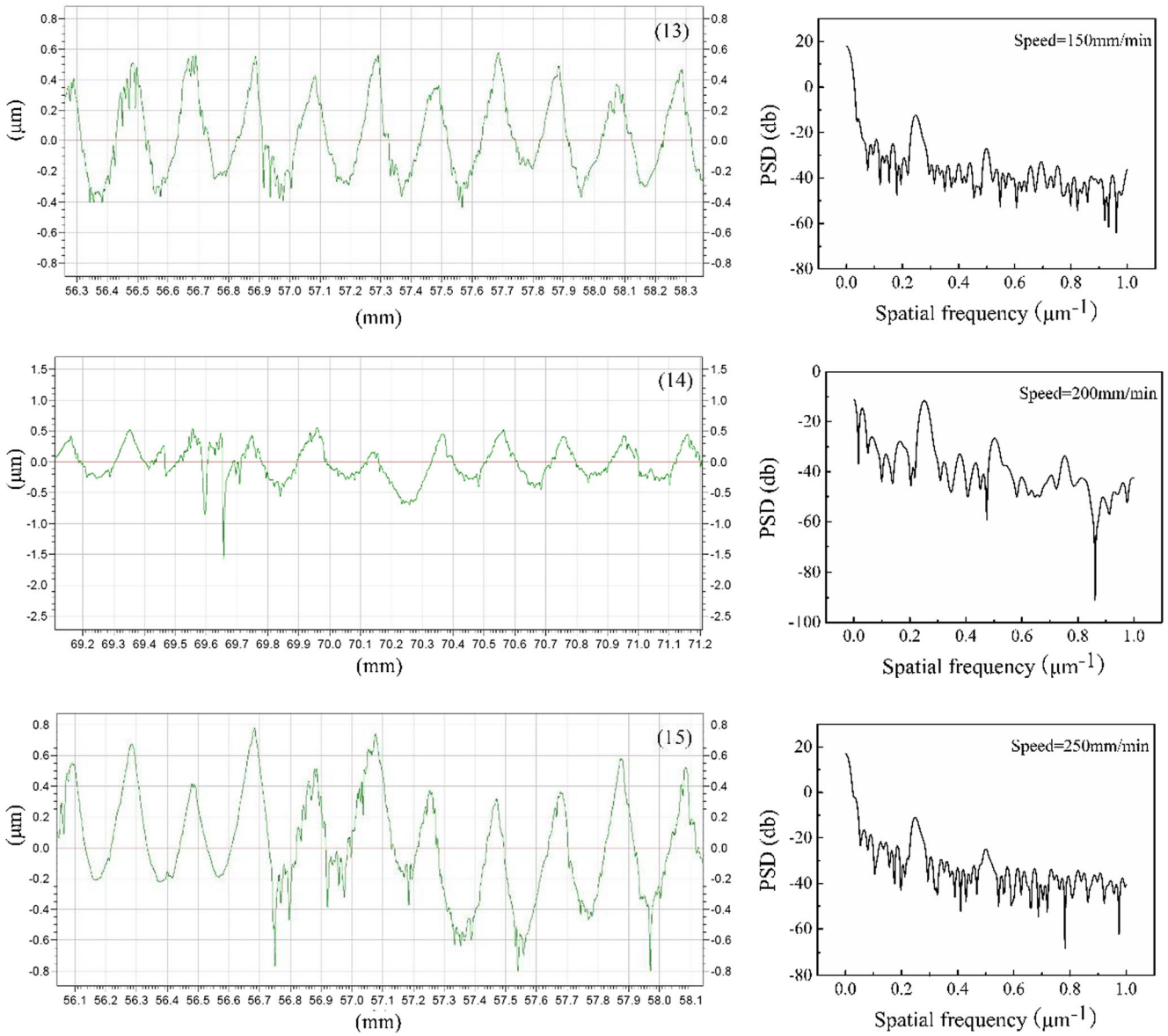

Fig. 14 Effect of speed on the surface topography (L) and the power spectral (R) density

was beginning to become larger. This meant that the surface topography of the periodic variation. At the same time, it can be seen from the surface topography graph that the distance between the peaks and valleys is starting to become big. When the feed rate was more than 0.4 mm, the distance between the peaks and valleys were larger than before milling. The surface roughness was therefore greater than that before milling. This was due to the introduction of new grooves on the part surface.

Burnishing speed had little effect on the surface topography and power spectral density (Fig. 14). It was worth noting that, when the speed reached about 200 mm/min, the magnitude of the power spectral density changed a little at low and high frequencies. This indicated that the surface texture is relatively uniform.

As shown in the surface topography graph (Fig. 15), the surface texture is uniform with the increase of the number of passes. When the number of passes reached five, the single peak shape of each contour was almost the same. Therefore, the magnitude of the power spectral density at high frequencies was almost unchanged. Compared the PSD profiles with the original PSD profile, it can be found that the burnishing pressure and feed rate were the dominant process parameters on the surface topography of the burnished workpiece. For all the workpieces, the analysis results of PSD profiles reveal that the LPB process significantly reduced the amplitude of the high frequency regions. Because surface roughness is closely related to the high frequency component of the surface topography, this effect can be regarded as a direct consequence of the reductions in surface roughness.

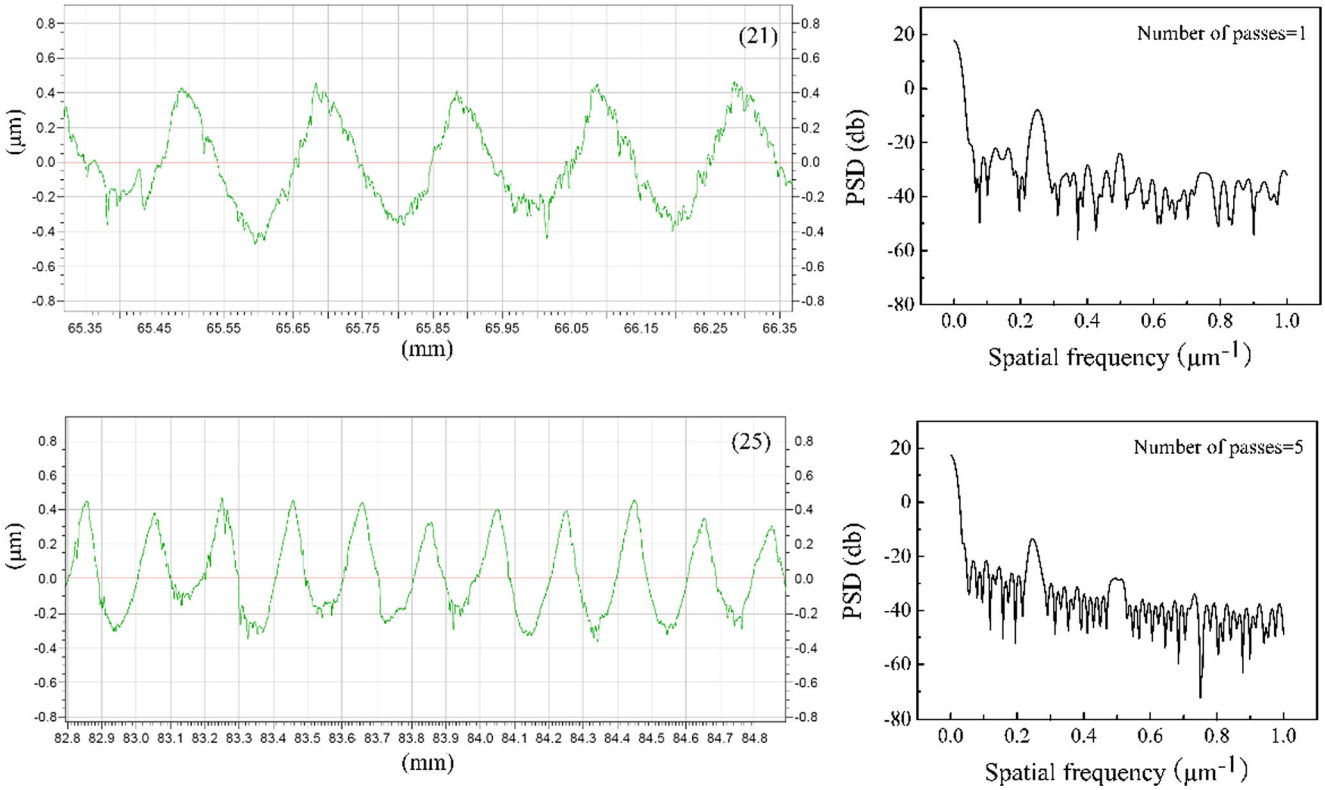

Fig. 15 Effect of number of passes on the surface topography (L) and the power spectral (R) density

4 Conclusions

Low plasticity burnishing was used to improve surface integrity of TA2 alloy. The effects of the burnishing parameters (pressure, speed, feed rate, and number of passes) on surface integrity characteristics were investigated. The following conclusions can be drawn:

- High burnishing pressure not only reduces the surface roughness but also improves high surface microhardness as well as generates high compressive residual stresses.
- Small feed rate has a positive effect on the surface roughness. There exists an optimal feed rate for obtaining the maximum surface microhardness and surface residual stress. The minimum surface roughness of 0.057 (Ra) is obtained at the feed rate of 0.05 mm.
- Burnishing speed has little influence on the surface roughness and surface microhardness. However, deep compressive residual stresses can be obtained at lower burnishing speed. The maximum residual stress of −501 Mpa is obtained at the speed of 150 mm/min.
- Burnishing with four passes is capable of decreasing the surface roughness by 64 % and increasing the surface microhardness by 45 %. More burnishing passes are more effective in increasing the compressive residual stress.
- Burnishing pressure and feed rate have the dominant effects on the surface topography of the burnished workpiece. Power spectral density of surface topography shows that the surface topography is cyclical at high frequencies. The periodicity of the surface topography is significant at high burnishing pressure with a low feed rate and high burnishing pressure.

Acknowledgments This work was supported by NSFC (51525501, 51321004).

References

1. Gharbi F, Sghaier S, Al-Fadhalah KJ, Benameur T (2011) Effect of ball burnishing process on the surface quality and microstructure properties of AISI 1010 steel plates. J Mater Eng Perform 20(6):903–910
2. Zhang T, Bugtai N, Marinescu ID (2014) Burnishing of aerospace alloy: a theoretical–experimental approach. J Manuf Syst 37:472–478
3. Luca L, Neagu-Ventzel S, Marinescu I (2005) Effects of working parameters on surface finish in ball-burnishing of hardened steels. Precis Eng 29(2):253–256
4. Okada M, Suenobu S, Watanabe K, Yamashita Y, Asakawaa N (2015) Development and burnishing characteristics of roller burnishing method with rolling and sliding effects. Mechatronics 29: 110–118
5. Rao DS, Hebbar HS, Komaraiah M, Kempaiah UN (2008) Investigations on the effect of ball burnishing parameters on surface hardness and wear resistance of HSLA dual-phase steels. Mater Manuf Process 23(3):295–302

6. Loh NH, Tam SC, Miyazawa S (1989) Statistical analyses of the effects of ball burnishing parameters on surface hardness. Wear 129(2):235–243
7. Abdulstaar M, Mhaede M, Wollmann M, Wagner L (2014) Investigating the effects of bulk and surface severe plastic deformation on the fatigue, corrosion behaviour and corrosion fatigue of AA5083. Surf Coat Technol 254:244–251
8. Hamadache H, Zemouri Z, Laouar L, Dominiak S (2014) Improvement of surface conditions of 36CrNiMo6 steel by ball burnishing process. J Mech Sci Technol 28(4):1491–1498
9. Sequera A, Fu CH, Guo YB, Wei XT (2014) Surface integrity of Inconel 718 by ball burnishing. J Mater Eng Perform 23(9):3347–3353
10. Zay K, Maawad E, Brokmeier HG, Genzel C (2011) Influence of mechanical surface treatments on the high cycle fatigue performance of TIMETAL 54M. Mater Sci Eng A 528(6):2554–2558
11. Gill CM, Fox N, Withers PJ (2008) Shakedown of deep cold rolling residual stresses in titanium alloys. J Phys D Appl Phys 41(17):174005
12. Prevéy PS, Cammett JT (2004) The influence of surface enhancement by low plasticity burnishing on the corrosion fatigue performance of AA7075-T6. Int J Fatigue 26(9):975–982
13. Rodríguez A, de Lacalle LNL, Celaya A, Lamikiz A, Albizuri J (2012) Surface improvement of shafts by the deep ball-burnishing technique. Surf Coat Technol 206(11):2817–2824
14. Yen YC, Sartkulvanich P, Altan T (2005) Finite element modeling of roller burnishing process. CIRP Ann Manuf Technol 54(1):237–240
15. Sayahi M, Sghaier S, Belhadjsalah H (2013) Finite element analysis of ball burnishing process: comparisons between numerical results and experiments. Int J Adv Manuf Technol 67(5-8):1665–1673
16. Mohammadi F, Sedaghati R, Bonakdar A (2014) Finite element analysis and design optimization of low plasticity burnishing process. Int J Adv Manuf Technol 70(5-8):1337–1354
17. Fu CH, Guo YB, McKinney J, Wei XT (2012) Process mechanics of low plasticity burnishing of Nitinol alloy. J Mater Eng Perform 21(12):2607–2617
18. Avilés R, Albizuri J, Rodríguez A, de Lacalle LL (2013) Influence of low-plasticity ball burnishing on the high-cycle fatigue strength of medium carbon AISI 1045 steel. Int J Fatigue 55:230–244
19. Gharbi F, Sghaier S, Morel F, Benameur T (2015) Experimental investigation of the effect of burnishing force on service properties of AISI 1010 steel plates. J Mater Eng Perform 24(2):721–725
20. Mhaede M (2012) Influence of surface treatments on surface layer properties, fatigue and corrosion fatigue performance of AA7075 T73. Mater Des 41:61–66